Journal of Structural Geology 32 (2010) 342–349

Contents lists available at ScienceDirect

Journal of Structural Geology

journal homepage: www.elsevier.com/locate/jsg

Rheology and microstructure of synthetic halite/calcite porphyritic aggregates in torsion

F.O. Marques*, L. Burlini, J.-P. Burg

Department of Geosciences, Swiss Federal Institute of Technology (ETH-Zürich), CH-8092 Zurich, Switzerland

ARTICLE INFO

Article history:
Received 14 May 2009
Received in revised form
11 December 2009
Accepted 4 January 2010
Available online 11 January 2010

Keywords:
Torsion experiments
Two-phase (composite) aggregate
Halite (rock salt)
Calcite
Rheology
Microstructure

ABSTRACT

Polymer jacketed porphyritic samples of 70% halite + 30% coarse calcite were subjected to torsion deformation to investigate the effects of a mixture of coarse calcite on the microstructure and mechanical properties of a two-phase aggregate. The experiments were run at 100 and 200 °C, a confining pressure of 250 MPa, and a constant shear strain rate of 3E-4 s^{-1}. Ultimate strengths of single-phase halite synthetic aggregates at 100 and 200 °C were ca. 32 and 8 Nm, respectively, and of the two-phase aggregate 39 and 18 Nm, respectively; this shows that the two-phase aggregate was much stronger, especially at 200 °C. Stepping strain rate tests show that the two-phase aggregate behaved as power-law viscous, with stress exponents of ca. 19 and 13 at 100 °C at 200 °C, respectively. From these high exponents, we infer that the active deformation mechanisms were not efficient enough to rapidly relax the applied stress. Halite stress exponents at 100 and 200 °C are typically much lower, in the order of 4–6, which means that the calcite porphyroclasts were obstacles to halite plastic flow and hampered stress relaxation. The drop of the stress exponent with temperature indicates that the main deformation mechanism(s) was temperature sensitive.

Matrix halite deformed plastically, while calcite rotated rigidly or deformed in a brittle fashion, with grain size reduction by fracturing (e.g. bookshelf and boudinage). We conclude that halite was softer than calcite in the investigated temperature range. Strain was homogeneous at the sample scale but not at the grain scale where the foliation delineated by plastically flattened halite contoured the rigid calcite clasts. The microstructures experimentally produced at 100 and 200 °C are very similar and find their counterparts in natural mylonites: rolling structures, σ and δ porphyroclast systems, bookshelf and boudinage in brittle calcite porphyroclasts, and ductile y and c' micro shear bands in the halite matrix.

1. Introduction

A major task of geoscientists has been to construct models that can explain the behaviour of the complex and heterogeneous lithosphere, while capturing its effective large-scale rheological behaviour. The fundamental models are the constitutive equations built from laboratory rock experimental data (e.g. Weertman's equation, Weertman and Weertman, 1975). Although much experimental work has been done, a better knowledge of the mechanical properties of the lithospheric constituents is still lacking, in particular for the mechanical properties of composites, albeit natural rocks are essentially polymineralic aggregates.

The mechanical and microstructural behaviour of polymineralic rocks can be described by three end-member types (e.g. Handy, 1990): (1) strong minerals form a load-bearing framework; (2) two or more minerals with low relative strengths control bulk rheology; (3) one very weak mineral governs bulk rheology, while the stronger minerals form porphyroclasts. Deforming rocks exhibit, at all scales, complex rheological responses ranging from strong quasi-rigid-like- to weak quasi-fluid-like-effective behaviour, as a function of temperature, stress, strain rate, fluids and/or rock composition. In many cases, both behaviours are found in the same deformed rock as, for example, in porphyritic granites deformed in greenschist facies conditions, where "hard" feldspar porphyroclasts are enclosed (in low concentration, little interaction) in a "soft" plastically deformed (fine grained) matrix of quartz and mica. Similarly, we investigate the effects of adding a (coarse, mostly equant grains) strong phase (quasi-rigid-like) to a weak (finer grained) plastic matrix (quasi-fluid-like) on the overall behaviour of a composite aggregate. This is still an open and relevant question because the solid-state rheology of rocks depends to a great extent on the

* Corresponding author. Present address: Departamento Geologia and CGUL-IDL, Faculdade Ciências, Universidade Lisboa, 1749-016 Lisboa, Portugal. Tel.: +351 217500000; fax: +351 217500064.
E-mail addresses: fernando.ornelas@erdw.ethz.ch, fomarques@fc.ul.pt (F.O. Marques).

0191-8141/$ – see front matter © 2010 Elsevier Ltd. All rights reserved.
doi:10.1016/j.jsg.2010.01.001

relative proportions of weak and strong minerals, and their shape and distribution. The use of mixed strong and weak phases poses a practical problem for experimental simulations, because in the laboratory most common natural ductile matrices (calcite or quartz) do not deform plastically at low temperatures typical of the greenschist facies, the conditions very common to many ductile shear zones involving the plastic deformation of calcite and quartz. In trying to overcome this problem, we used as analogues (after e.g. Williams et al., 1977; Hobbs et al., 1982; Wilson, 1983; Burg and Wilson, 1987) a soft plastic (at low temperature and laboratory strain rates) matrix made of halite and hard coarse grain calcite clasts to investigate the behaviour and mechanical properties of a two-phase porphyritic synthetic aggregate with contrasting rheology and behaviour of the constituents. In order to assess the contribution of calcite to the rheology of the halite/coarse calcite aggregate, we compare it with the experimental behaviour of synthetic single-phase halite aggregates deformed under similar experimental conditions. Up to now, most low temperature work with 2-phase aggregates has been done in axial compression and low strain. However, a great deal of deformation of rocks takes place in ductile shear zones dominated by simple shear (e.g. Ramsay, 1967; Burg, 1999). It is thus very advantageous to make available microstructural and mechanical data resulting from simple shear deformation to large strains. With this aim, we carried out torsion experiments to simulate strain in shear zones and achieve high shear strains typical of natural high shear strain zones (mylonites).

Previous experimental work has used 2-phase aggregates to analyze the effect of randomly distributed hard grains on the mechanics of rock salt (e.g. Price, 1982; Bloomfield and Covey-Crump, 1993; Kawamoto and Shimamoto, 1998), or to gain a better understanding of mylonites (e.g. Ross et al., 1987; Jordan, 1987), or to study foliation development in quartz-mica rocks in pure shear flow (e.g. Williams et al., 1977; Hobbs et al., 1982; Wilson, 1983; Burg and Wilson, 1987).

Price (1982), on the basis of triaxial compression tests, observed relatively small strength increases with increase in anhydrite content up to 50% at 200 °C, 200 MPa (from 14.1 MPa differential stress for 100% halite, to 18.5 MPa for 50% halite), and much larger increases in strength above 50% anhydrite content (from 18.5 MPa for 50% halite, to 84.2 MPa for 0% halite). Jordan (1987) used both axially symmetric compression and simple shear, and concluded that the strength of the bulk aggregate decreases as the foliation intensifies. Ross et al. (1987) used simple shear to deform halite-anhydrite synthetic aggregates at 300 °C and 200 MPa, and concluded that the aggregate strength strongly increased with anhydrite content. Bloomfield and Covey-Crump (1993) and Covey-Crump et al. (2006) have studied the behaviour of mixtures, at different proportions of halite and calcite in uniaxial compression tests. Bruhn and Casey (1997) deformed aggregates of calcite and anhydrite in compression and found that for the equal proportions aggregate the strength is lower than for the pure end-member aggregate. Barnhoorn et al. (2005) deformed a similar type of aggregate, to very large strain in torsion, and found that the admixture of a second phase can lead to strain localization, whilst the single-phase end-members deformed homogeneously. This is particularly interesting since anhydrite undergoes a switch from dislocation to diffusion creep from low to high strain, but this did not lead to strain localization (Heidelbach et al., 2001). Delle Piane et al. (2009) deformed aggregates of fine-grained calcite and mica in torsion, where mica behaved as hard phase and calcite as soft. At high strain calcite was segregated in high strain zones where deformation localized.

Common to all previous works mentioned above is the similar grain size of the constituents and the use of metal jackets. In the present experiments the samples were porphyritic, with calcite porphyroclasts up to two times coarser than the halite groundmass. This places the used samples in end-member type 3 of Handy (1990). As discussed below, this could be in part responsible for the differences in microstructure and rheology observed between the present and previous experimental results. In addition, the use of metal jackets makes it very difficult to compare rheology with the present experiments, because polymer jackets do not interfere with sample resistance to flow.

With the present experiments, we intended to find answers to the following questions: (1) what is the behaviour of each phase in the aggregate? (2) How do they interfere? (3) What are the differences in mechanical properties between the two-phase aggregate and single-phase halite? What is the role of calcite? (4) Does strain localize in the halite/coarse calcite aggregate?

We did not investigate the internal deformation of calcite because we could not discriminate the inherited deformation (strains developed during natural formation of the Carrara marble, and later crushing and cold isostatic pressing to make the synthetic aggregate) and the deformation produced during the experimental torsion tests. We did not investigate the deformation mechanisms of halite in torsion, because this was done previously at the ETH-Zürich (Armann, 2008; Wenk et al., 2009). However, we analysed the microstructure and evaluated the mechanical properties of the composite aggregate, which were sufficient to show that; (i) halite behaved plastically in contrast to the brittle behaviour of calcite; (ii) the two-phase synthetic aggregate was much stronger than the single-phase halite aggregate under the chosen experimental conditions; and (iii) despite the low concentration of calcite in the aggregate, type 3 end-member, the porphyroclasts can dominate the strength of the aggregate.

2. Materials and methods

2.1. Sample preparation

The specimens were synthesized by cold pressing a mixture of 70% halite (analytical grade powder with grain size <500 μm) and 30% of coarse calcite (ground from Carrara marble and sieved to a grain size between 500 and 1000 μm). This volume fraction was chosen to represent common porphyritic rocks where phenocrysts do not interact (cf. Fig. 1) during deformation. The synthetic aggregate was then hot isostatically stored at 200 °C for one week. After this procedure, the sample showed a slightly anisotropic texture made of a honeycomb-like structure of halite crystals surrounding coarse calcite defining a perceptible foliation (Fig. 1), and a porosity of ca. 1%. Under crossed nicols (inset Fig. 1), it is clear that the contact between halite grains is marked by calcite dust (mostly) and fluid inclusions. Fluid inclusions are also observed along healed fractures, possibly formed during cold pressing. Cylindrical samples 15 mm in diameter were cored and oven-dried at 110 °C and atmospheric pressure for at least 24 h before the tests. Because halite is soluble in water, drilling was made with compressed air and polishing was carried out dry. The samples were inserted in a 0.5 mm thick and 15 mm inner diameter polymer jacket (very soft polyethylene and polytetrafluorethylene) to assess the mechanical properties of the aggregate free of the mechanical and chemical jacket influences. In order to try and reach higher shear strain at 200 °C, we occasionally used copper jackets, but only for the analysis of the microstructure.

2.2. Deformation apparatus and boundary conditions

The experiments were conducted in a Paterson rig, an apparatus based on a standard gas-medium, high-pressure and high-temperature triaxial deformation machine, to which an additional module has been added that allows rotary shear of a cylindrical specimen (Paterson and Olgaard, 2000). In torsion experiments, approximated

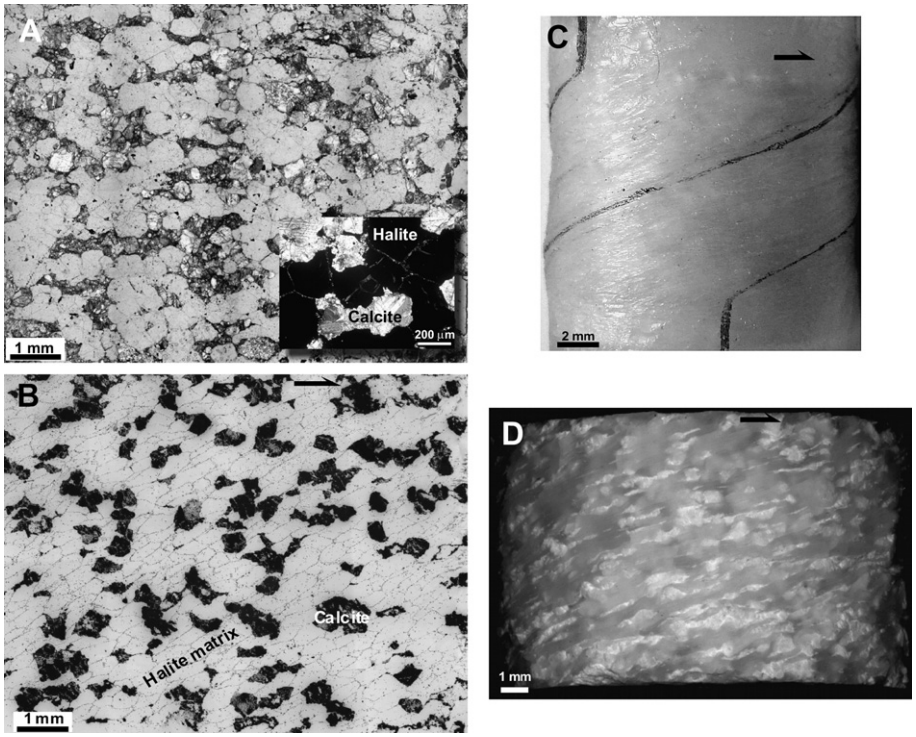

Fig. 1. A – transmitted light image of initial stage. Inset to show that grain contacts are marked by (mostly) calcite dust and fluid inclusions, which allow visualization of plastic strain of halite. Fluid inclusions also mark healed fractures (e.g. honeycomb structure inside grain in the centre of inset), likely formed during cold isostatic pressing. Background image with nicols crossed to ¼ λ; inset is full crossed nicols. B – inverted colour transmitted light micrograph image of sample deformed to $\gamma = 1$, at 100 °C. Note the homogeneous character of deformation in the plastic halite matrix, at the scale of the sample, defining a shear foliation oblique to the shear plane. In detail, stretching of halite grains is not homogeneous; stretching tends to be greater in domains where calcite grains are smaller or less abundant, and smaller where calcite grains are bigger or more concentrated. Also note that calcite grains do not interact appreciably. C and D – images of the overall aspect of sample with and without polymer jacket after deformation to $\gamma = 3$ at 100 °C. Note the homogeneous character of deformation at the sample scale. Marker lines on jacket surface were initially straight and along the cylinder axis.

simple shear deformation occurs locally at any given position in the sample. The shear strain γ and shear strain rate $\dot{\gamma}$ increase linearly from 0 along the central axis of the sample to a maximum value at the outer circumference. The $\dot{\gamma}$ at any radius are calculated from the angular displacement rates using Eq. (3) in Paterson and Olgaard (2000). The experimental γ and $\dot{\gamma}$ mentioned are, therefore, maximum values. The temperature distributions were regularly calibrated so that the temperature variation across the sample was never more than ±1 °C. The experiments were conducted at 100 and 200 °C, at 250 MPa confining pressure and at constant angular displacement rate corresponding to a $\dot{\gamma} = 3\text{E-}4\ s^{-1}$ up to $\gamma = 6$.

Stepping strain rate tests ($\dot{\gamma}$ from 1E-5 s^{-1} to 2E-3 s^{-1}) were run to determine the dependence of flow strength on $\dot{\gamma}$. The response of the internal torque M to a variation in angular displacement rate ($\dot{\theta}$) yields the stress exponent $n(n = \Delta \ln\dot{\theta}/\Delta \ln M)$(Eq. (12) of Paterson and Olgaard, 2000), which can give an indication of the active deformation mechanism.

3. Experimental results

3.1. Microstructure

The experiments were characterized by homogeneous deformation at the sample scale (no strain localization), despite the 30 volume % of coarse calcite in the aggregate (Fig. 1). However, deformation at the grain scale was heterogeneous and occasionally localized in ductile micro shear bands. Halite grains deformed plastically and homogeneously away from strong calcite clasts, and plastically but heterogeneously near calcite clasts. Calcite deformed mostly in a brittle fashion, with significant grain size reduction by fracture.

Microstructures experimentally produced at 100 and 200 °C are very similar (Figs. 2 and 3) and find their counterparts in natural mylonites (Lister and Price, 1978; Berthé et al., 1979; Burg et al., 1981; Choukroune et al., 1987; Gaudemer and Tapponnier, 1987; Marques et al., 2007); this is the case of (i) rolling structures (van den Driessche and Brun, 1987; Marques and Coelho, 2001; Marques and Burlini, 2008; Marques and Coelho, 2003; Taborda et al., 2004; Marques et al., 2005) and δ porphyroclast systems (Passchier and Simpson, 1986; Bose and Marques, 2004) – synthetic rotation of calcite clasts deduced from drag tails of small calcite grains, calcite dust and fluid inclusions, from distortion of halite grains around calcite clasts, and from the high angle of many elongated clasts relative to the shear foliation (not common in the initial stage); (ii) ductile synthetic micro shear bands parallel to the bulk shear plane (Fig. 2a); (iii) synthetic ductile Riedel shears–strain localization along synthetic ductile micro shear bands dipping ca. 20° towards shear sense, where the foliation became sigmoidal and closely spaced in the middle of the shear band (Fig. 3b); (iv) bookshelves (Fig. 2) – micro normal faults (antithetic to applied shear), with variable dip opposite to sense of shear, cutting across calcite grains, with block rotation and separation responsible for a great deal of the observed grain size reduction; (v) boudins (Fig. 2) – breaking and separation of calcite grains healed by flow of the plastic halite matrix; (vi) grain size reduction of calcite by fracturing (Figs. 2 and 3); (vii) antithetic ductile micro shear bands resulting from rotation of neighbouring porphyroclasts (Fig. 3a).

3.2. Mechanical properties

Stress/strain curves (Fig. 4a) were constructed to evaluate the sample responses in terms of resistance to flow (shear stress), to an

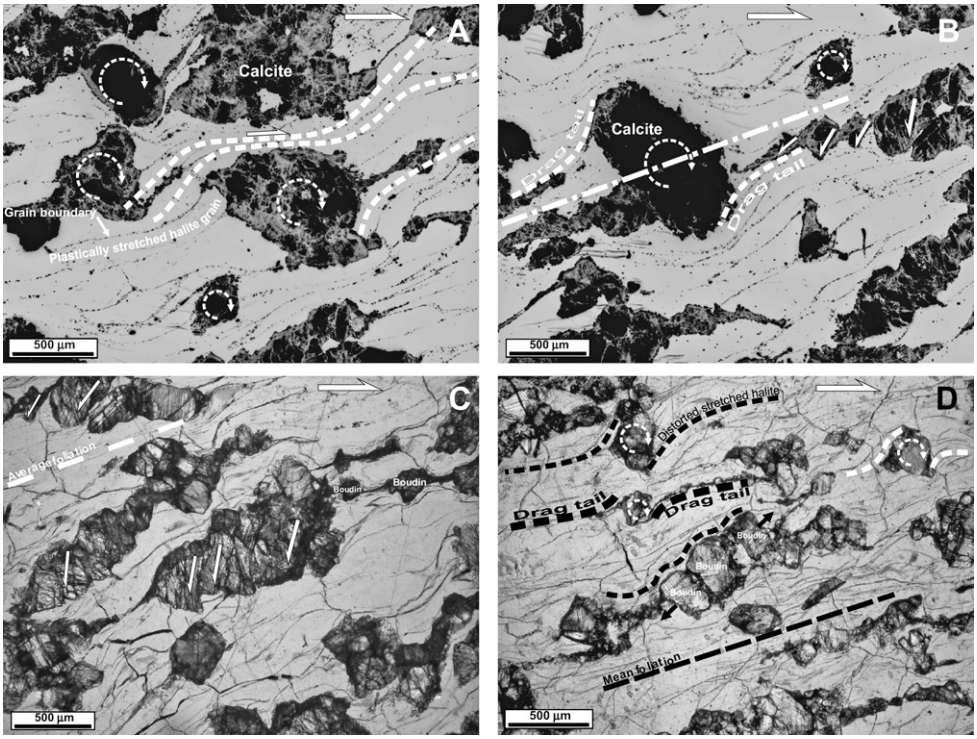

Fig. 2. Inverted colour transmitted light micrograph images of samples deformed to $\gamma = 3$, at 100 °C. A – note the inhomogeneous character of deformation in the plastic halite matrix, at the scale of the grain. Halite was plastically stretched and distorted to conform to the more rigid calcite clasts. Note the high angle of many calcite clasts relative to the mean foliation, a feature not common in the initial stage where most clasts were aligned horizontally and defining a perceptible foliation. Drag and distortion of tails made of small calcite grains also indicate synthetic rotation of calcite clasts. Locally, strain localized, the foliation became sigmoidal and halite grains much more stretched, with development of a ductile synthetic micro shear band parallel to the shear plane. Arrowed open circles indicate clast rotation deduced from drag patterns of tails and halite grains. B – drag and distortion of tails made of calcite dust and fluid inclusions indicate synthetic rotation of calcite clasts. The grain in the centre right shows bookshelf fracturing and disaggregation, with daughter clast synthetic rotation shown by decreasing dip of micro faults away from the parent clast. C – most calcite grains in the image show bookshelf fracturing and disaggregation (including boudinage) that led to considerable grain size reduction. D – Sample deformed to $\gamma = 3$, at 200 °C. The calcite grain in the centre is elongated parallel to the expansion axis of simple shear (marked by black arrows) and was boudinaged with separation healed by halite inflow. Arrowed open circles mark clast rotation inferred from drag tails (made of small calcite grains) and distortion of plastic halite grains. Clast and dragged tail define a δ-clast.

applied constant $\dot{\gamma}$ (Tables 1 and 2). All curves show elastic loading until a yield, although at different stress levels and with different slopes. The initial gradients prior to yielding reflect the elastic shear moduli of the specimens, which for the two-phase aggregates was ca. 1575 MPa, and for the one-phase aggregate was ca. 640 MPa. Yield was followed by strain hardening in all samples. Constant flow stress after hardening occurred at 100 °C in all but one of the two-phase aggregates and in one-phase halite at 200 °C. Only one experiment at 100 °C out of many at 100 and 200 °C showed strain softening after peak torque (Fig. 4a).

Despite general similarities, some significant differences characterize each experiment at 100 °C: (i) early strain hardening in halite/coarse calcite samples was much steeper than for halite; hence yield for the samples containing calcite was not as evident as for halite; (ii) strain hardening in the halite/coarse calcite sample gradually vanished, and flow eventually reached constant flow stress around $\gamma = 1.5$; (iii) in one experiment, peak torque at ca. 41 Nm was followed by strain softening till ca. 39 Nm; (iv) in the single-phase halite sample, early moderate hardening was followed by constant flow stress between $\gamma = 1.7$ and $\gamma = 2.7$. This stage was followed by moderate strain hardening until jacket failure at $\gamma = 5$; (v) The two-phase aggregate was stronger than the single-phase halite aggregate, especially until $\gamma = 2.7$.

The stepping strain rate data for the 2-phase aggregate is best fit by a power-law curve. Taking logarithms of torque and $\dot{\gamma}$, the plot shown in Fig. 4b is obtained. From the equations, two stress exponents, $n = 19$ and 13, are thus determined for 100 and 200 °C, respectively.

In contrast to the 100 °C experiment, one and two-phase samples showed clear yield at 200 °C (Fig. 4a), although at quite different torque levels. The elastic shear modulus was ca. 1270 MPa, which is significantly lower than the ca. 1575 MPa at 100 °C. The smaller slope of the (prior to yielding) curve for the single halite aggregate shows that the elastic shear modulus is significantly smaller than for the composite aggregate. In both aggregates at 200 °C, yield was followed by steep hardening till about $\gamma = 0.5$. Steep hardening in the two-phase aggregate gradually changed into gentle hardening, and eventually constant flow stress at about $\gamma = 3$ and peak torque of ca. 17 Nm. In the single-phase halite aggregate, hardening quickly vanished and constant flow stress initiated at about $\gamma = 0.5$ and peak torque of ca. 8.5 Nm.

4. Discussion

With the present experiments, we intended to answer the following questions.

4.1. What is the behaviour of each phase in the aggregate?

The experiments show that halite deformed plastically, in agreement with what is reported in Armann (2008) and Wenk et al. (2009), and calcite rotated rigidly or fractured, possibly along planes of weakness inherited from the cold pressing stage to make the aggregate. We could not find demonstrative evidence for plastic behaviour of the calcite crystals. From the experimental results we

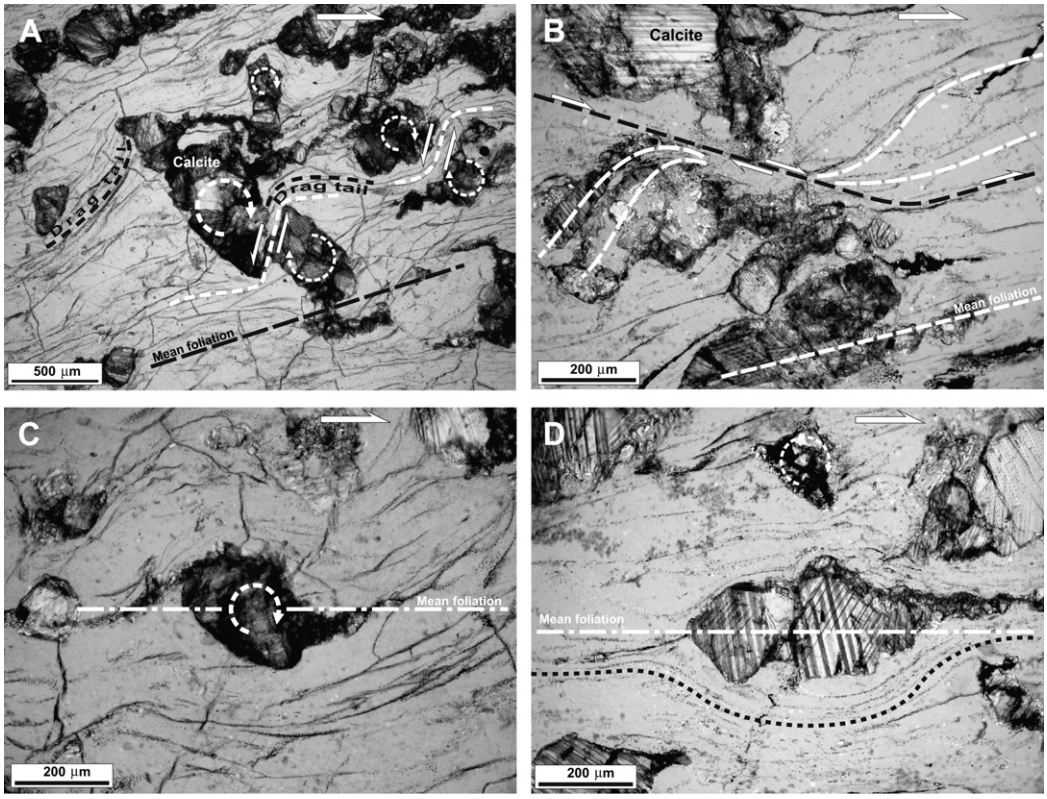

Fig. 3. Inverted colour transmitted light micrograph images of samples deformed to $\gamma = 3$, at 200 °C. A – arrowed open circles mark clast rotation inferred from drag tails and distortion of plastic halite grains. Neighbouring clasts rotating in the same sense induced the formation of antithetic ductile micro shear bands. B – Close up of synthetic ductile micro shear band (ductile Riedel or *C′*). C – close up of calcite clast and dragged tail defining a δ-clast. D – close up of calcite clast and stair-stepping tails defining a σ-clast.

infer that calcite was stronger than halite under the experimental conditions.

4.2. How do halite and calcite interfere?

Plastically deforming halite crystals had to contour the rigid calcite clasts and were dragged by the synthetic rotation of calcite clasts. From the stress/strain curves, especially at 100 °C, we infer that the bigger the clasts the stronger the aggregate (see discussion below), because of greater obstacle to halite plastic flowage.

4.3. What are the differences in mechanical properties between the two-phase and single-phase halite aggregates? What is the role of calcite porphyroclasts?

At 100 °C, the single-phase halite aggregate underwent strain hardening until $\gamma = 5$, whereas the two-phase aggregate flowed at constant stress short after $\gamma = 1$ until the end of the run. However, the composite aggregate was much stronger than the single aggregate in the early stages, but tended to converge to the curve of single halite with strain, because of halite strain hardening in the single-phase aggregate. Our interpretation is that big and rigid calcite clasts worked as obstacles to halite plastic flowage (thus making the aggregate stronger), and that calcite grain size reduction by fracturing balanced with halite work hardening to produce the early constant flow stress. It could not be due to the halite behaviour, because single-phase halite underwent significant strain hardening till $\gamma = 5$. According to Wenk et al. (2009), halite hardening can be due to decrease in {110} slip, especially beyond $\gamma = 3$. The effect of the calcite clasts on the mechanical properties of the composite aggregate was also shown by the elastic shear modulus, which was much higher for the composite aggregate. We attribute this increased shear modulus to the role of calcite porphyroclasts in strengthening the bulk behaviour of the aggregate.

At 200 °C, the two-phase aggregate was more than twice stronger than the single-phase, but the latter reached a constant flow stress much earlier, in contrast to the strain hardening of the two-phase aggregate until $\gamma = 5$ and contrary to the 100 °C experiment. Because there was a switch in behaviour (hardening) between one and two-phase aggregates with temperature, we infer that temperature played a role in the mechanical behaviour of the aggregates. Since we were not able to decipher any change in the behaviour of calcite with temperature (rotation and fracturing at both 100 and 200 °C), we can only attribute the changes in mechanical behaviour to halite; at 200 °C halite was flowing at constant flow stress before $\gamma = 1$, and at ca. 1/4 of the peak strength at 100 °C. It seems, therefore, that the weak resistance of halite at 200 °C was not immediately balanced by softening due to calcite grain size reduction. This seems to have happened at higher strain, when the flow of the composite aggregate at 200 °C showed a tendency to constant flow stress.

Stepping strain rate tests show how a rock specimen responds to the imposed variations in strain rate. The gradient is typically positive, which means that the rock hardens with increasing strain rate. The hardening rate (stress exponent n, typically positive) is a measure of the efficiency of active deformation mechanisms in relaxing the applied stress. It has been shown (e.g. Karato, 2008) that a relation can exist between n and the active deformation mechanism (e.g. diffusion or dislocation creeps). However, several mechanisms are usually active simultaneously. For instance, grain size reduction as in the present experiments must also be taken into account in the interpretation of the meaning of n, because grain size reduction is supposed to soften a rock and localize

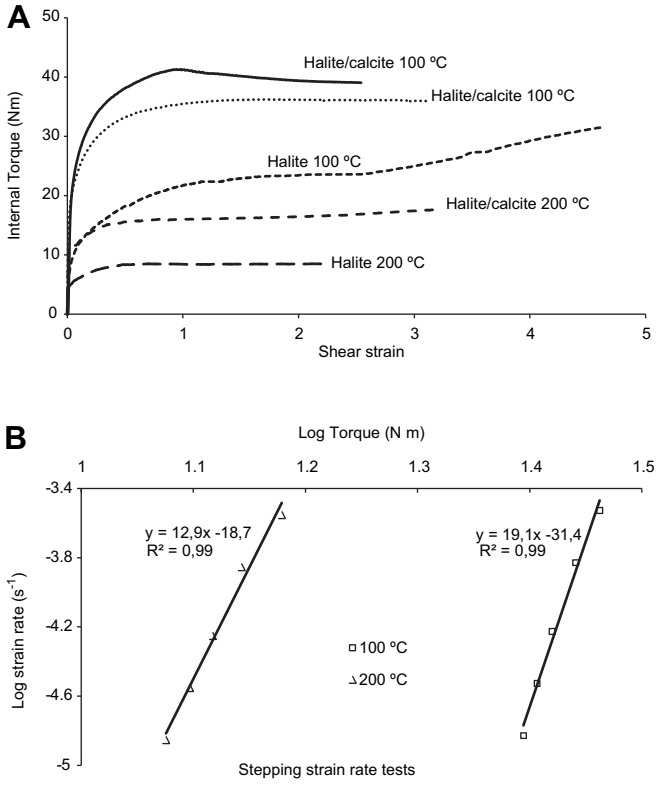

Fig. 4. Torque/strain curves for the halite/calcite and halite synthetic aggregates. A mixture of 30% calcite made the aggregate significantly stronger, at least until $\gamma = 3$ at 100 °C, and twice as strong at 200 °C. Note that the one and only experiment with strain softening occurred at 100 °C in the two-phase aggregate. The single-phase halite aggregate reached constant flow stress at low values of strain at 200 °C (in great contrast to experiments at 100 °C), and that it is still the weakest aggregate. Contrary to 100 °C, constant flow stress was first achieved by the single-phase halite aggregate at 200 °C. B – log/log graph showing the stepping strain rate curves used to deduce mechanical properties and the stress exponent n at 100 and 200 °C.

deformation. In rocks undergoing dynamic recrystallization, further care should be taken when trying to correlate n with a specific deformation mechanism because several mechanisms can be active at the same time. Mechanical softening may result from grain size reduction via brittle processes, which enhance the strain rate contribution of grain size sensitive mechanisms, such as diffusion creep, grain boundary sliding or superplasticity. We will not go into further details for the plastic deformation of halite and halite aggregates, which has been documented by previous work (Davidge and Pratt, 1964; Le Compte, 1965; Carter and Heard, 1970; Heard, 1972; Poirier, 1972; Guillopé and Poirier, 1979; Carter and Hansen, 1983; Wawersik and Zeuch, 1986; Horseman and Handin, 1990; Spiers et al., 1990; Senseny et al., 1992; Franssen, 1994; Spiers and Carter, 1998; Schléder and Urai, 2007; Armann, 2008; Wenk et al., 2009). In the present experiments the rigid behaviour of calcite porphyroclasts must be taken into account because n of single-phase halite aggregates varies from ca. 4 to 6, at 100 and 200 °C, respectively, in contrast to $n = 19$ and 13 for the two-phase aggregate at the same temperatures. We conclude that the presence of rigid, although rotating, inclusions hampered stress relaxation and was responsible for the high stress exponents. These rigid particles worked as obstacles to the free flow of the halite matrix, so making more difficult for the plastic matrix to relax the applied stress. Therefore, the rock hardened. In both single-phase halite and two-phase aggregates, n dropped significantly with temperature, which means that the active deformation mechanisms (or part of them) were temperature sensitive.

4.4. Does strain localize in the halite/coarse calcite aggregate?

Not at the scale of the sample. However, at the grain scale, deformation localized against calcite porphyroclasts. Rotation and heterogeneous distribution of calcite porphyroclasts induced the local formation of synthetic and antithetic ductile micro shear bands.

A question was raised by the experimental results: why was there clear yielding at 200 °C in comparison to the 100 °C experiments? A possible explanation is that, at low temperature, the elastic component predominated for longer because the rigid calcite clasts hampered plastic flowage. At 200 °C the elastic component vanished earlier, most probably because at this temperature halite was very weak. Also work hardening at 100 °C was steeper than at 200 °C, which makes the yielding point more conspicuous. We observed that calcite behaved in a brittle manner, but we could not quantify its contribution to the bulk behaviour or the difference in calcite brittle behaviour at 100 and 200 °C. Anyway, sharp yield points are characteristic of plastic behaviour, which suggests that at 200 °C the bulk behaviour was more plastic than brittle. Plastic behaviour has well defined strain rate sensitivity expressed by the stress exponent of power-law behaviour, whereas dry brittle behaviour is insensitive to strain rate (e.g. Rutter and Mainprice, 1978). Therefore, the stress exponents determined in the present work should reflect the cumulative effect of halite plastic behaviour and flow hampering imposed by calcite clasts.

Discussion of the present experimental results in view of the previous experimental work is not straightforward because we used: (i) porphyritic samples, at variance to previous work on equigranular aggregates; (ii) calcite, whose shape is in contrast to platy minerals (mostly mica) used in many of the previous works; (iii) very weak polymer jackets, in contrast to the strong metal jackets of previous studies; (iv) torsion, where equant grains rotate synthetically and generate drag structures, in contrast to axial compression where equant grains do not rotate or rotate both synthetically and antithetically. However, we can discuss the present results in the light of Einstein's theory of viscosity (Einstein, 1906) and of the results of Bloomfield and Covey-Crump (1993).

It is known sinceEinstein (1906) that the viscosity of a fluid increases with the amount of suspended rigid inclusions. Because halite macroscopically behaved under the experimental conditions like a fluid, a likely explanation for the increase in strength in the two-phase aggregate could be an increase in viscosity. However, viscosity is very sensitive to temperature. Therefore, despite the similar amount of calcite in the aggregate, the increase in strength (i.e. viscosity) also depended on temperature: 32–39 Nm at 100 °C, and 8–18 Nm at 200 °C. Einstein's equation is valid for spherical inclusions, and it applies only to suspensions that are sufficiently dilute and where there is no inclusion interaction. The present experiments were not that ideal; inclusions were not spherical and could, to a certain extent, interact, despite the used low calcite volume fraction.

Bloomfield and Covey-Crump (1993) showed that resistance to flow increased with calcite volume fraction in synthetic halite/calcite aggregates. They concluded that the calcite *contiguous* volume should be used, rather than the actual calcite volume fraction, to characterize the strength of the aggregates with respect to those of their component phases. However, the present experiments showed that contiguity changed with strain because calcite clasts rotated and fractured, and that contact surfaces changed orientation relative to applied stresses, thus changing stress propagation. Bloomfield and Covey-Crump (1993) called attention to the fact that contiguity can be zero or negligible (all calcite grains surrounded by halite) in samples with relatively low content of inclusions. In such cases, like in the present experiments, the problem could be reduced to that of a viscous fluid with suspended rigid inclusions. However, our experiments showed that this is not

Table 1
Experimental conditions and mechanical results.

Run	Sample	Temperature (K)	Jacket	Steady torque (Nm)	Strain rate (s^{-1})	Max. strain (γ)	Comments jacket failure	Other comments
P-911	Synthetic Halite	373	PE	NA	3.0E-04	5	Jacket failed 241 mn	
P-918	Synthetic Halite	373	PE	NA	SSR	NA	Halted before jacket fail	
P-925	Synthetic Halite	373	PTFE	NA	SSR	NA	Halted before jacket fail	
P-926	Synthetic Halite	473	PTFE	NA	SSR	NA	Halted before jacket fail	
P-951	Synthetic Halite	473	PTFE	NA	SSR	NA	Halted before jacket fail	
P-953	Synthetic Halite	573	PTFE	NA	SSR	NA	Halted before jacket fail	
P-1018	Synthetic Halite	473	PTFE	8.5	3.0E-04	2	Halted before jacket fail	
P-1068	Synthetic Halite	333	PEHD	NA	SSR	NA	Halted before jacket fail	
P-1070	Synthetic Halite	333	PEHD	NA	SSR	NA	Halted before jacket fail	
P-948	70% Hl + 30% Cc	373	PTFE	NA	3.0E-04	2.1	Halted before jacket fail	Slipped at 105 mn
P-949	70% Hl + 30% Cc	373	PTFE	NA	3.0E-04	1.2	Halted before jacket fail	Slipped at 60 mn
P-950	70% Hl + 30% Cc	373	PTFE	NA	3.0E-04	0.4	Halted at 22 mn	
P-952	70% Hl + 30% Cc	373	PE	36	3.0E-04	3.6	Halted at 180 mn	
P-954	70% Hl + 30% Cc	473	PTFE	18.8	3.0E-04	3.4	Halted before jacket fail	Slipped at 170 mn
P-955	70% Hl + 30% Cc	473	PTFE	NA	3.0E-04	0.4	Halted at 21 mn	
P-956	70% Hl + 30% Cc	373	PTFE	NA	3.0E-04	0.06	Halted at 3 mn	
P-957	70% Hl + 30% Cc	473	PTFE	NA	3.0E-04	0.06	Halted at 3 mn	
P-972	70% Hl + 30% Cc	373	PTFE	NA	3.0E-04	0.3	Halted at 15 mn	
P-973	70% Hl + 30% Cc	373	PTFE	NA	SSR	NA	Halted before jacket fail	
P-983	70% Hl + 30% Cc	373	PTFE	NA	3.0E-04	0.9	Halted at 46 mn	
P-984	70% Hl + 30% Cc	373	PTFE	NA	3.0E-04	1.1	Halted before jacket fail	Slipped at 56 mn
P-985	70% Hl + 30% Cc	473	PTFE	NA	SSR	NA	Halted before jacket fail	
P-1037	70% Hl + 30% Cc	473	Cu	NA	3.0E-04	2.7	Jacket failed at 133 mn	
P-1040	70% Hl + 30% Cc	473	PTFE	17.6	3.0E-04	3.6	Jacket failed 180 mn	
P-1041	70% Hl + 30% Cc	473	PTFE	NA	3.0E-04	1.2	Halted at 60 mn	
P-1044	70% Hl + 30% Cc	473	PTFE	NA	3.0E-04	1.8	Halted before jacket fail	Slipped after 90 mn
P-1064	70% Hl + 30% Cc	373	PEHD	41.3	3.0E-04	3.9	Jacket failed at 195 mn	Softening after peak torque

Hl – halite; Cc – calcite; PE – polyethylene; PTFE – polytetrafluorethylene; PEHD – polyethylene high density; Cu – copper; SSR – stepping strain rate test; NA – not applicable.

a valid approach, because strength (viscosity) also depended on temperature. Therefore, a more complete explanation must be sought on the differential behaviour of calcite and halite. Because calcite did not show a visible difference in behaviour at 100 or 200 °C, we deduce that the exponential softening of halite with temperature played a major role, because then the rheological contrast between the two phases increased.

The present experimental results in torsion using very soft polymer jackets, especially for the high-pressure tests, differ markedly from those of Price (1982); 30% of coarse calcite content made the 2-phase aggregate much stronger than single-phase halite at identical temperature. Jordan (1987) concluded that the strength of the bulk aggregate decreases as the foliation intensifies. The present experiments do not show this behaviour at 100 °C; despite the development of a shear foliation that progressively rotated towards the shear plane in the single-phase halite aggregate, the torque/strain curves showed strain hardening, at least to $\gamma = 5$ (see also Armann, 2008; Wenk et al., 2009). Regarding the microstructure and simple shear experiments, Jordan (1987) also warned that the shear sense could be erroneously deduced from σ- and δ-clasts. In the present experiments we found that all shear criteria were consistent with the applied torsion. However, the shape of calcite grains seems to have controlled the type of porphyroclast system; δ-clasts developed mostly from equant grains, and σ-clasts developed mostly from elongated grains. Because most grains were roughly equant, rolling structures were very common microstructures (e.g. Marques and Burlini, 2008). Elongated grains can stay for longer with the longest axis sub-parallel to the shear plane (e.g. Marques and Coelho, 2003) and so be more prone to develop into σ-clasts. Ross et al. (1987) deformed halite-anhydrite synthetic aggregates at 300 °C and 200 MPa. Therefore, we cannot compare the mechanical behaviour, because the present experiments were run in torsion at lower temperatures. Regarding the microstructural development, the present experimental results look very similar to the photomicrographs shown by Ross et al. (1987), despite the higher temperature of their experiments with a different hard phase. Kawamoto and Shimamoto (1998) studied the strength profile of calcite–halite mixtures at high-temperature and low confining pressure by shearing experiments. Comparison cannot be made with the present experiments for which pressure is one order of magnitude higher and temperature 3–6 times lower.

According to Handy (1990), the bulk rheology of the aggregate should be governed by the weaker phase. However, despite the small concentration of calcite and thus small grain interaction (not the strong framework required for type 1), the two-phase aggregate was much stronger than the one-phase aggregate of the weakest mineral. This was even more evident at 200 °C, possibly because the rheological contrast between phases increases with temperature; halite is much weaker at 200 °C than at 100 °C, while calcite strength does not change appreciably at the tested temperatures and strain rates.

Table 2
Stepping strain rate data (polymer jackets).

100 °C		200 °C	
Log internal torque	Log strain rate	Log internal torque	Log strain rate
1.39	−4.83	1.08	−4.85
1.41	−4.53	1.10	−4.55
1.42	−4.23	1.12	−4.25
1.44	−3.83	1.14	−3.85
1.46	−3.53	1.18	−3.55

Acknowledgments

The experiments were carried out in the Rock Deformation Lab, ETH-Zürich (ETH 0-12422-97, LZ 3392). FOM acknowledges a sabbatical fellowship by FCT (Portugal) and a guest fellowship by the ETH-Zürich. This is a contribution to research project GEOMODELS2006 (PTDC/CTE-GIN/66281/2006) rejected by FCT,

Portugal. Reviews by D. Mainprice and C. Wilson helped to improve the quality of this manuscript.

References

Armann, M., 2008. Microstructural and Textural Development in Synthetic Rocksalt Deformed in Torsion. PhD thesis, ETH-Zürich, Switzerland.

Barnhoorn, A., Bystricky, M., Kunze, K., Burlini, L., Burg, J.-P., 2005. Strain localisation in bimineralic rocks: experimental deformation of synthetic calcite–anhydrite aggregates. Earth and Planetary Science Letters 240, 748–763.

Berthé, D., Choukroune, P., Jegouzo, P., 1979. Orthogneiss, mylonite and non coaxial deformation of granites: the example of the South Armorican Shear Zone. Journal of Structural Geology 1, 31–42.

Bloomfield, J.P., Covey-Crump, S.J., 1993. Correlating mechanical data with microstructural observations in deformation experiments on synthetic two-phase aggregates. Journal of Structural Geology 15, 1007–1019.

Bose, S., Marques, F.O., 2004. Controls on the geometry of tails around rigid circular inclusions: insights from analogue modelling in simple shear. Journal of Structural Geology 26, 2145–2156.

Bruhn, D.F., Casey, M., 1997. Texture development in experimentally deformed two-phase aggregates of calcite and anhydrite. Journal of Structural Geology 19, 909–925.

Burg, J.-P., 1999. Ductile structures and instabilities: their implication for Variscan tectonics in the Ardennes. Tectonophysics 309, 1–25.

Burg, J.-P., Wilson, C.J.L., 1987. Deformation of two phase systems with contrasting rheologies. Tectonophysics 135, 199–205.

Burg, J.-P., Iglesias, M., Laurent, P., Matte, P., Ribeiro, A., 1981. Variscan intra-continental deformation: the Coimbra–Cordoba shear zone (SW Iberian Peninsula). Tectonophysics 78, 161–177.

Carter, N.L., Hansen, F.D., 1983. Creep of rocksalt. Tectonophysics 92, 275–333.

Carter, N.L., Heard, H.C., 1970. Temperature and rate dependent deformation of halite. American Journal of Sciences 269, 193–249.

Choukroune, P., Gapais, D., Merle, O., 1987. Shear criteria and structural symmetry. Journal of Structural Geology 9, 1347–1350.

Covey-Crump, S.J., Schofield, P.F., Daymond, M.R., 2006. Using neutrons to investigate changes in strain partitioning between the phases during plastic yielding of calcite + halite composites. Physica B 385–386, 946–948.

Davidge, R.W., Pratt, P.L., 1964. Plastic deformation and work-hardening in NaCl. Physica Status Solidi 6, 759–776.

Delle Piane, C., Wilson C. J. L., Burlini L., 2009. Dilatant plasticity in high-strain experiments on calcite-muscovite aggregates. *Journal of Structural Geology*. doi: 10.1016/j.jsg.2009.03.005.

van den Driessche, J., Brun, J.P., 1987. Rolling structures at large shear strains. Journal of Structural Geology 9, 691–704.

Einstein, A., 1906. Eine neue bestimmung der moleküldimensionen. Annalen der Physik 19, 289–306, with a correction in vol. 34, p. 591 (1911).

Franssen, R.C.M.W., 1994. The rheology of synthetic rocksalt in uniaxial compression. Tectonophysics 233, l–40.

Gaudemer, Y., Tapponnier, P., 1987. Ductile and brittle deformations in the northern Snake Range, Nevada. Journal of Structural Geology 9, 159–180.

Guillopé, M., Poirier, J.P., 1979. Dynamic recrystallization during creep of single-crystalline halite: an experimental study. Journal of Geophysical Research 84, 5557–5567.

Handy, M.R., 1990. The solid-state flow of polymineralic rocks. Journal of Geophysical Research 95, 8647–8661.

Heard, H.C., 1972. Steady state flow in polycrystalline halite at pressure of two kilobars. In: Heard, H.C., Borg, J.Y., Carter, N.L., Raleigh, C.B. (Eds.), Flow and Fracture of Rocks, Geophysical Monograph Series 16. AGU, Washington, DC, pp. 191–209.

Heidelbach, F., Stretton, I.C., Kunze, K., 2001. Texture development of polycrystalline anhydrite experimentally deformed in torsion. International Journal of Earth Sciences 90, 118–126.

Hobbs, B.E., Means, W.D., Williams, P.F., 1982. The relationship between foliation and strain: an experimental investigation. Journal of Structural Geology 4, 411–428.

Horseman, S.T., Handin, J., 1990. Triaxial-compression tests on rocksalt at temperatures from 50 to 200 °C and strain rates from 10^{-4} to 10^{-9}/s. American Geophysical Union, Geophysical Monographs 56, 103–110.

Jordan, P.G., 1987. The deformational behaviour of bimineralic limestone-halite aggregates. Tectonophysics 135, 185–197.

Karato, S.-I., 2008. Deformation of Earth Materials: An Introduction to the Rheology of the Solid Earth. Cambridge University Press, New York. 463p.

Kawamoto, E., Shimamoto, T., 1998. The strength profile for bimineralic shear zones: an insight from high-temperature shearing experiments on calcite–halite mixtures. Tectonophysics 295, 1–14.

Le Compte, P., 1965. Creep in rock salt. Journal of Geology 73, 469–484.

Lister, G.S., Price, G.P., 1978. Fabric development in a quartz–feldspar mylonite. Tectonophysics 49, 37–78.

Marques, F.O., Burlini, L., 2008. Rigid inclusions rotate in geologic materials as shown by torsion experiments. Journal of Structural Geology 30, 1368–1371.

Marques, F.O., Coelho, S., 2001. Rotation of rigid elliptical cylinders in viscous simple shear flow: analogue experiments. Journal of Structural Geology 23, 609–617.

Marques, F.O., Coelho, S., 2003. 2-D shape preferred orientations of rigid particles in transtensional viscous flow. Journal of Structural Geology 25, 841–854.

Marques, F.O., Schmid, D.W., Andersen, T.B., 2007. Applications of inclusion behaviour models to a major shear zone system: the Nordfjord-Sogn detachment zone in Western Norway. Journal of Structural Geology 29, 1622–1631.

Marques, F.O., Taborda, R., Antunes, J., 2005. 2-D rotation of rigid inclusions in confined bulk simple shear flow: a numerical study. Journal of Structural Geology 27, 2171–2180.

Passchier, C.W., Simpson, C., 1986. Porphyroclast systems as kinematic indicators. Journal of Structural Geology 8, 831–844.

Paterson, M.S., Olgaard, D.L., 2000. Rock deformation tests to large shear strains in torsion. Journal of Structural Geology 22, 1341–1358.

Poirier, J.P., 1972. High temperature creep of single crystalline sodium chloride. Philosophical Magazine 26, 713–725.

Price, R.H., 1982. Effects of anhydrite and pressure on the mechanical behaviour of synthetic rocksalt. Geophysical Research Letters 9, 1029–1032.

Ramsay, J.G., 1967. Folding and Fracturing of Rocks. McGraw-Hill, New York, 568 pp.

Ross, J.V., Bauer, S.J., Hansen, F.D., 1987. Textural evolution of synthetic anhydrite-halite mylonites. Tectonophysics 140, 307–326.

Rutter, E., Mainprice, D., 1978. The effect of water on the stress relaxation of faulted and unfaulted sandstone. Pure and Applied Geophysics 111, 634–654.

Schléder, Z., Urai, J.L., 2007. Deformation and recrystallization mechanisms in mylonitic shear zones in naturally deformed extrusive Eocene-Oligocene rocksalt from Eyvanekey plateau and Garmsar hills (central Iran). Journal of Structural Geology 29, 241–255.

Senseny, P.E., Hansen, F.D., Russell, J.E., Carter, N.L., Handin, J., 1992. Mechanical behavior of rock salt: phenomenology and micromechanisms. International Journal of Rock Mechanics 29, 363–378.

Spiers, C.J., Carter, N.L., 1998. Microphysics of rocksalt flow in nature. In: Aubertin, M. (Ed.), The Mechanical Behaviour of Salt: Proceedings of the Fourth Conference Trans Tech Publication Series on Rock and Soil Mechanics, vol. 22. Trans Tech Publication, pp. 115–128.

Spiers, C.J., Schutjens, P.M.T.M., Brzesowsky, R.H., Peach, C.J., Liezenberg, J.L., Zwart, H.J., 1990. Experimental determination of constitutive parameters governing creep of rocksalt by pressure solution. In: Knipe, R.J., Rutter, E.H. (Eds.), Deformation Mechanisms, Rheology and Tectonics. Geological Society of London, Special Publications, vol. 54, pp. 215–227.

Taborda, R., Antunes, J., Marques, F.O., 2004. 2-D Rotation behavior of a rigid ellipse in confined viscous simple shear: numerical experiments using FEM. Tectonophysics 379, 127–137.

Wawersik, W.R., Zeuch, D.H., 1986. Modelling and mechanistic interpretation of creep of rocksalt below 200 °C. Tectonophysics 121, 125–152.

Weertman, J., Weertman, J., 1975. High temperature creep of rock and mantle viscosity. Annual Review of Earth Planet and Planetary Sciences 3, 293–315.

Wenk, H. -R., Armann, M., Burlini, L., Kunze, K., Bortolotti, M., 2009. Large strain shearing of halite: experimental and theoretical evidence for dynamic texture changes. *Earth and Planetary Science Letters*, doi:10.1016/j.epsl.2009.01.036.

Williams, P.F., Means, W.D., Hobbs, B.E., 1977. Development of axial plane slaty cleavage and schistosity in experimental and natural materials. Tectonophysics 42, 139–158.

Wilson, C. J. L., 1983. Foliation and strain development in ice-mica models. In: M. Etheridge and S. Cox (Eds.), *Deformation Processes in Tectonics. Tectonophysics* 92, 93–122.